Article

Neuron

Disrupted Prefrontal Regulation of Striatal Subjective Value Signals in Psychopathy

Highlights

- Ventral striatal subjective value signals are amplified in incarcerated psychopaths
- Medial cortico-striatal intrinsic connectivity is weak in psychopathic individuals
- Cortico-striatal regulation of striatal activation is disrupted in psychopathy
- Diminished cortico-striatal regulation is associated with more criminal convictions

Authors

Jay G. Hosking, Erik K. Kastman, Hayley M. Dorfman, ..., Kent A. Kiehl, Joseph P. Newman, Joshua W. Buckholtz

Correspondence

jhosking@fas.harvard.edu (J.G.H.), joshua_buckholtz@harvard.edu (J.W.B.)

In Brief

Psychopaths are notorious for their criminal behavior and poor self-control, but underlying neural mechanisms remain unresolved. Using fMRI in incarcerated offenders, Hosking et al. show that regulatory cortico-striatal connectivity is weakened in psychopathy, driving heightened striatal value encoding during decision making.

Hosking et al., 2017, Neuron *95*, 221–231
July 5, 2017
http://dx.doi.org/10.1016/j.neuron.2017.06.030

CellPress

Neuron
Article

Disrupted Prefrontal Regulation of Striatal Subjective Value Signals in Psychopathy

Jay G. Hosking,[1,*] Erik K. Kastman,[1] Hayley M. Dorfman,[1] Gregory R. Samanez-Larkin,[7] Arielle Baskin-Sommers,[2] Kent A. Kiehl,[3] Joseph P. Newman,[4] and Joshua W. Buckholtz[1,5,6,8,*]
[1]Department of Psychology, Harvard University, 52 Oxford St., Cambridge, MA 02138, USA
[2]Department of Psychology, Yale University, 2 Hillhouse Ave., New Haven, CT 06520, USA
[3]MIND Institute, 1101 Yale Blvd NE, Albuquerque, NM 87106, USA
[4]Department of Psychology, University of Wisconsin-Madison, 1202 W Johnson St., Madison, WI 53706, USA
[5]Center for Brain Science, Harvard University, 52 Oxford St., Cambridge, MA 02138, USA
[6]Department of Psychiatry, Massachusetts General Hospital, 55 Fruit Street, Boston, MA 02144, USA
[7]Department of Psychology and Neuroscience, Duke University, 417 Chapel Dr., Durham, NC 27708, USA
[8]Lead Contact
*Correspondence: jhosking@fas.harvard.edu (J.G.H.), joshua_buckholtz@harvard.edu (J.W.B.)
http://dx.doi.org/10.1016/j.neuron.2017.06.030

SUMMARY

Psychopathy is a personality disorder with strong links to criminal behavior. While research on psychopathy has focused largely on socio-affective dysfunction, recent data suggest that aberrant decision making may also play an important role. Yet, the circuit-level mechanisms underlying maladaptive decision making in psychopathy remain unclear. Here, we used a multi-modality functional imaging approach to identify these mechanisms in a population of adult male incarcerated offenders. Psychopathy was associated with stronger subjective value-related activity within the nucleus accumbens (NAcc) during inter-temporal choice and with weaker intrinsic functional connectivity between NAcc and ventromedial prefrontal cortex (vmPFC). NAcc-vmPFC connectivity strength was negatively correlated with NAcc subjective value-related activity; however, this putative regulatory pattern was abolished as psychopathy severity increased. Finally, weaker cortico-striatal regulation predicted more frequent criminal convictions. These data suggest that cortico-striatal circuit dysregulation drives maladaptive decision making in psychopathy, supporting the notion that reward system dysfunction comprises an important neurobiological risk factor.

INTRODUCTION

Crime is estimated to cost the United States more than a trillion dollars a year (Anderson, 1999). Even apart from its traumatizing effects on victims, the enormous economic burden associated with criminal behavior renders it a critical target for scientific investigation. One particularly robust predictor of criminal behavior and recidivism is psychopathy. Psychopathy is a personality disorder comprising both interpersonal-affective and impulsive-antisocial symptoms; these include superficial charm and egocentric grandiosity, callousness and diminished empathy, disinhibition, heightened sensation seeking, and persistent antisocial behavior (Viding et al., 2014). Psychopathy is notoriously difficult to treat (Brazil et al., 2016), and intervention efforts are hampered by our limited understanding of the cognitive and neurobiological underpinnings of the disorder.

Neuroscientific work to date has largely focused on the interpersonal-affective dimension of psychopathy. These studies have found relatively consistent evidence for amygdala and ventromedial prefrontal cortex (vmPFC) dysfunction, which is thought to underlie aberrant fear learning, moral decision making, and empathic responsiveness in the disorder (Blair, 2008; Koenigs et al., 2011; Viding et al., 2014). Morphological findings indicate decreased amygdala and vmPFC gray matter volume, and lower vmPFC cortical thickness, in psychopathy (Ermer et al., 2012; Yang and Raine, 2009). Likewise, psychopaths show reduced recruitment of amygdala and vmPFC during fear conditioning and moral decision making (Birbaumer et al., 2005; Glenn et al., 2009; Harenski et al., 2010), blunted amygdala responsiveness during affective perspective taking (Decety et al., 2013a), and weaker vmPFC engagement in response to empathogenic (Decety et al., 2013b) and facial emotion stimuli (Carré et al., 2013; Viding et al., 2014). Reduced functional and structural connectivity between amygdala and vmPFC has also been reported in psychopathy (Motzkin et al., 2011). Notably, there is some evidence that the observed relationships between psychopathy, task-related brain activity, and vmPFC-amygdala connectivity are driven by the interpersonal-affective features of the disorder (Carré et al., 2013; Decety et al., 2014; Hyde et al., 2014). This observation accords well with functional and structural brain imaging work in youth and adolescents with callous-unemotional traits (Blair, 2013), which are considered by some to be a developmental precursor of the interpersonal-affective symptoms in adult psychopathy (Frick and Viding, 2009). On the whole, these findings make a compelling case that social and affective deficits in psychopathy arise from cortico-limbic circuit dysfunction (Blair, 2013; Viding et al., 2014).

While the neurobiological mechanisms underlying interpersonal-affective symptoms in psychopathy are coming increasingly

into focus, less is known about the impulsive-antisocial dimension of the disorder. While some consider interpersonal-affective features to be most central to the construct of psychopathy, impulsive-antisocial symptoms appear to have much stronger links to many of the most problematic behaviors associated with the disorder, such as physical aggression, criminal behavior, and substance abuse (Skeem and Mulvey, 2001; Walters, 2003). A series of recent functional and neuroreceptor imaging studies, performed largely in community volunteers, raises the possibility that such symptoms may be driven by aberrant reward processing within the meso-cortico-limbic dopamine system. We have shown previously that high impulsive-antisocial scores on a self-report psychopathic trait inventory predicted elevated amphetamine-induced dopamine release and heightened reward anticipation-related activity within the nucleus accumbens (NAcc) (Buckholtz et al., 2010). The association between impulsive-antisocial behavior and reward anticipation-related blood-oxygen-level dependent (BOLD) signal has been replicated in both healthy volunteers and in adolescents with externalizing (i.e., impulsive-antisocial) symptoms (Bjork et al., 2010, 2012; Carré et al., 2013). Likewise, several groups have found evidence for increased striatal gray matter volume in psychopathic offenders (Glenn et al., 2010), particularly those with a history of impulsive violence (Schiffer et al., 2011). Taken together, these studies suggest that impulsive-antisocial behavior in psychopathy is associated with exaggerated dopamine transmission and increased functional reactivity to rewards within the striatum.

While these findings are suggestive, several critical questions remain unresolved. First, with psychopathy's prevalence estimated at 1% in the general population (Coid et al., 2009), relatively few community volunteers would meet forensic criteria for psychopathy. The generalizability of findings derived from convenience samples to individuals with clinically significant levels of psychopathy, and who manifest chronic and consequential self-control deficits, therefore remains uncertain. Second, previous studies of striatal function in psychopathy have employed experimental paradigms that lack a meaningful decision-making component. This makes it difficult to conclusively link aberrant striatal function in psychopathic individuals to the kinds of decision-making biases that could plausibly predispose antisocial behavior. Finally, the circuit-level mechanisms that underlie striatal hyper-reactivity in psychopaths remain unknown. While some groups have reported reduced vmPFC-amygdala connectivity in psychopathic individuals (Motzkin et al., 2011), it is unclear whether regulatory medial cortico-striatal connectivity is disrupted as well. This question is particularly salient given evidence that "top-down" prefrontal inputs to NAcc (Sesack and Grace, 2010) regulate striatal response and choice behavior during cost-benefit decision making (Buckholtz, 2015; Ferenczi et al., 2016; van den Bos et al., 2014). Currently, the nature of cortico-striatal connectivity in psychopathy and its link to choice-related striatal value signaling remain unknown.

Given the importance of cortico-striatal connectivity for regulating reward-related striatal dopamine release, striatal activity, and choice behavior, we hypothesized that striatal hyper-reactivity in psychopathic individuals is driven by a disruption in the cortical regulation of striatal information processing. Specifically, we predicted that participants with higher levels of psychopathy would show stronger striatal subjective value-related responses during cost-benefit decision making and weaker intrinsic cortico-striatal connectivity. We further predicted that, consistent with previous work suggesting that medial prefrontal cortex negatively regulates striatal dopamine release and population activity (Ferenczi et al., 2016), value-related striatal fMRI signal would be negatively correlated with intrinsic cortico-striatal connectivity. Finally, we predicted that the negative relationship between striatal activation and cortico-striatal connectivity would be progressively abolished with increasing psychopathy severity.

To test these predictions, we administered an intertemporal choice (i.e., delay-discounting) task to 49 male incarcerated offenders at two medium-security prisons, while utilizing a mobile fMRI scanner to assess both task-related activation and resting-state functional connectivity. Psychopathy was measured with the Psychopathy Checklist-Revised (PCL-R) (Hare and Neumann, 2008), which differentiates interpersonal-affective ("Factor 1") and impulsive-antisocial ("Factor 2") components. Given prior associations between the impulsive-antisocial traits of psychopathy and reward-related striatal BOLD (Buckholtz et al., 2010), we expected that this dimension of psychopathy would better track striatal activity during intertemporal decision making, compared to interpersonal-affective aspects of the disorder.

RESULTS

Psychopathy Is Positively Associated with Striatal Subjective Value-Related BOLD Signal

Prior work indicates that NAcc is especially important for representing the subjective value of choice options during cost-benefit decision making generally (Bartra et al., 2013) and during intertemporal choice specifically (Peters and Büchel, 2011). To examine the relationship between psychopathy and NAcc value coding, we first derived each participant's discount rate (k) using a hyperbolic discount utility function and softmax choice rule (see STAR Methods). k values ranged from 0.0001 to 0.1116 (mean = 0.0125, standard deviation = 0.0257). Using these subject-specific k values, we estimated the subjective value (SV) of each of the two choice options (i.e., sooner-but-smaller or larger-but-later) presented to participants on each trial. For each trial, SV for the two options was summed; we then modeled this summed SV as a trial-wise parametric modulator of BOLD activity at the time of choice. We chose to model the sum of subjective values based in part on work in primates suggesting that NAcc neuron firing is specifically sensitive to this decision variable (Cai et al., 2011). Based on the evidence described above indicating an association between psychopathic traits and NAcc dysregulation, we extracted BOLD signal estimates for each subject using an anatomical NAcc region of interest (ROI) derived from a large connectivity-based striatal parcellation study (Choi et al., 2012).

First, we confirmed that NAcc was sensitive to trial-wise variation in subjective value, consistent with prior reports (Peters and Büchel, 2011) (Figure 1A; small-volume corrected with bilateral NAcc ROI: $p_{FWE(peak\text{-}level)}$ = 0.043, peak t value = 3.55, peak MNI coordinate: 12, 12, −6, whole-brain analysis: peak MNI coordinate: 4, 12, 0; peak t value = 5.94, k = 304, $p_{FDR(peak\text{-}level)}$ = 0.029). Next, our correlation analysis using signal extracted

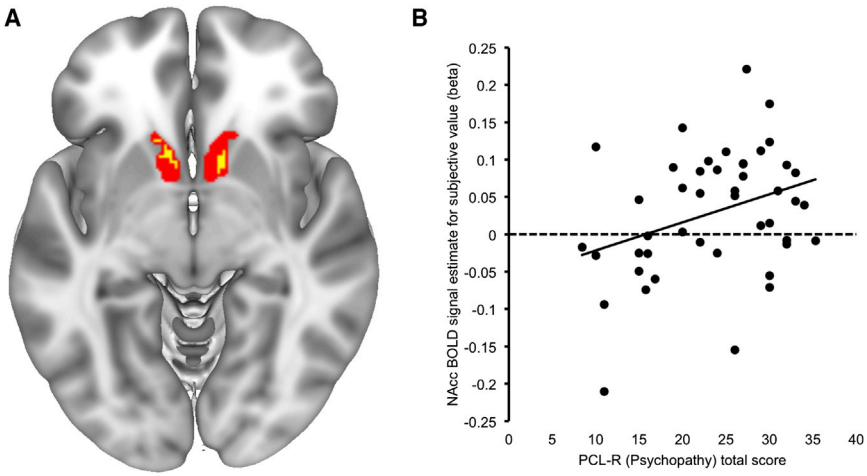

Figure 1. Subjective Value-Related BOLD Activity in the NAcc Tracks Psychopathy Scores

(A) The main effect of subjective value across all participants (yellow shading) is overlaid on the nucleus accumbens (NAcc) region of interest (ROI; red shading) used to extract BOLD signal estimates for individual difference analyses (Choi et al., 2012). Small-volume corrected cluster (with bilateral NAcc ROI): $p_{FWE(peak\text{-}level)}$ = 0.043, peak t value = 3.55, peak MNI coordinate: 12, 12, −6. Whole-brain cluster: peak MNI coordinate: 4, 12, 0; peak t value = 5.94, k = 304, $p_{FWE(peak\text{-}level)}$ = 0.029.

(B) Scatterplot illustrates the significant positive correlation between psychopathy and subjective value-related BOLD signal within right NAcc.

from NAcc ROIs revealed a significant positive relationship between inmates' total psychopathy scores and SV-related BOLD signal in right NAcc (Figure 1; r = 0.335, p = 0.024; left NAcc: r = 0.03, p = 0.846). The relationship between PCL-R total score and NAcc BOLD signal remained significant using robust regression (t = 2.19, p = 0.034) and after removing for high-influence cases (t = 2.75, p = 0.009). Examining the two PCL-R factors separately revealed a significant association with Factor 1 (interpersonal-affective) scores (Figure S2; r = 0.397, p = 0.007); by contrast, the relationship with Factor 2 (impulsive-antisocial) scores was considerably weaker (r = 0.271, p = 0.075). However, a Williams test for differences in dependent correlations was not significant (p = 0.366), limiting our ability to make a strong claim about factor-selective associations to striatal SV-BOLD signal. In sum, these data show that higher levels of psychopathy (i.e., PCL-R total score) were associated with heightened subjective value-related activation within NAcc during choice behavior in incarcerated criminal offenders. This finding is consistent with prior work in community volunteers and suggests that reward-related striatal hyper-reactivity both generalizes to a clinically relevant population and is evident during consequential decisions about rewards. Notably, and contrary to our *a priori* hypothesis, the effect size for this relationship was larger for the interpersonal-affective dimension of psychopathy.

Weaker Intrinsic Cortico-striatal Connectivity in Psychopathy

The analysis above suggested that striatal subjective value signaling during intertemporal decision making is relatively dysregulated in psychopathy. Less clear, however, is the source of this dysregulation. Preclinical and human data highlight a prominent role for prefrontal cortex in regulating reward-related striatal DA release and population activity. The striatum receives robust, topographically organized afferent input from multiple sectors of PFC (Haber et al., 1995). Glutamate release from these cortico-striatal terminals has been shown to inhibit stimulus-dependent release of dopamine at meso-striatal synapses (Sesack and Grace, 2010). This prefrontal modulation of striatal function is thought to be one means through which higher-order value representations maintained in PFC (e.g., information about goals, costs, and context) guide adaptive action selection (Buckholtz, 2015; Ferenczi et al., 2016; Jimura et al., 2013; Quiroz et al., 2016; van den Bos et al., 2014). We therefore hypothesized that striatal hyper-reactivity in psychopathy may be due, in part, to compromised prefrontal regulation of striatal activity. To test this hypothesis, we examined the relationship between psychopathy and cortico-striatal resting-state functional connectivity (rsFC). Striatal rsFC networks were identified across all participants, using the same anatomical NAcc ROI in which we found a significant association between PCL-R scores and striatal SV-related BOLD (Figure 2A, Table S1, and Figure S3; see "Main effects of resting-state NAcc functional connectivity" below for additional results).

We then performed a random-effects whole-brain regression analysis using participants' PCL-R scores as a predictor of striatal rsFC. Consistent with the notion of compromised cortico-striatal connectivity in psychopathy, higher PCL-R scores were associated with weaker connectivity between NAcc and a cluster with center of mass in vmPFC (Figures 2B and 2C; peak at MNI 6, 52, −4; BA 10, Z = 3.84, p_{FDR} = 0.017, k = 246). This analysis also revealed a positive correlation between PCL-R scores and NAcc-precuneus rsFC (MNI −24, −44, 50; Z = 3.90, p_{FDR} = 0.039, k = 220). All results remained significant via robust regression analysis (i.e., using connectivity values extracted from suprathreshold vmPFC cluster described above; t = −4.58, p < 0.001) and after controlling for age and substance abuse history (see Table S2). Both Factor 1 and Factor 2 showed significant negative associations to NAcc-vmPFC rsFC (p < 0.005 for both factors via OLS regression using parameter estimates extracted from significant cluster in striatal rsFC-PCLR total regression SPM; p < 0.01 via robust regression with age and substance abuse covariates). Taken together, these findings show that psychopathy is associated with reduced cortico-striatal connectivity, such that participants with higher PCL-R scores showed weaker functional coupling between the nucleus accumbens and ventromedial prefrontal cortex.

Cortico-striatal Modulation of Striatal SV-Related BOLD

The finding that psychopaths are characterized by a combination of heightened striatal reactivity and weakened cortico-striatal

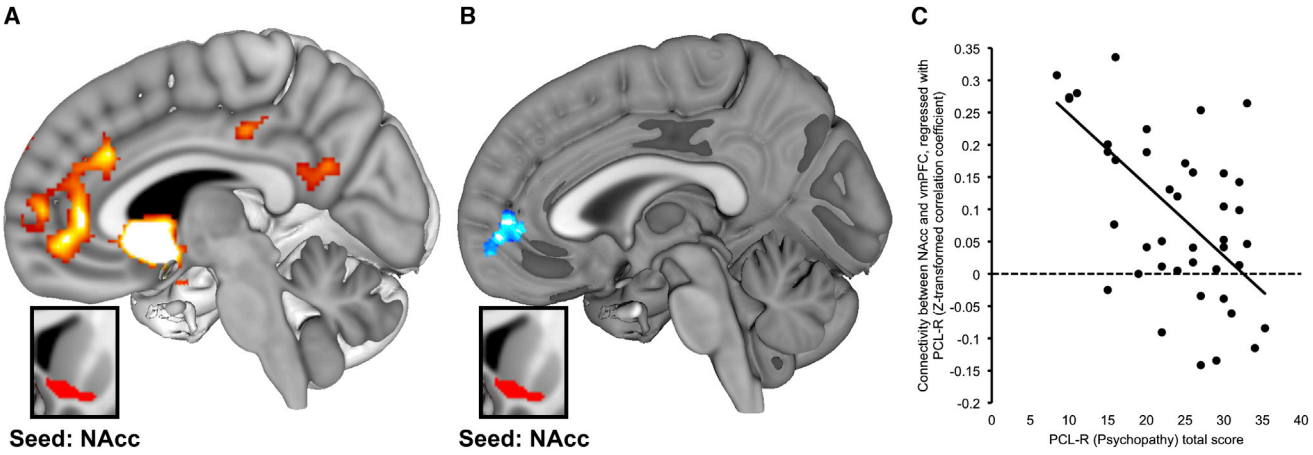

Figure 2. Psychopathy Is Associated with Weaker Intrinsic Connectivity between NAcc and vmPFC

(A) SPM depicts regions demonstrating significant main effect of functional connectivity with right NAcc seed across all participants ($p_{FDR} < 0.05$; seed region shown in inset box; see Table S1 and Figure S3).

(B) SPM depicts regions where the magnitude of functional connectivity to right NAcc (inset box) differed as a function of PCL-R total scores. Specifically, higher psychopathy scores were associated with weaker NAcc connectivity to vmPFC ($p_{FDR} < 0.05$; blue shading).

(C) Scatterplot illustrates the negative correlation between psychopathy scores and NAcc functional connectivity with the vmPFC cluster identified in (B).

connectivity is particularly interesting in light of anatomical data showing that ventral striatum is a target of substantial projections from prefrontal cortex (Haber et al., 1995). Indeed, there is considerable evidence that these cortico-striatal afferents comprise a crucial means of regulating ventral striatal population activity, DA release, and reward decision making (Buckholtz, 2015; Ferenczi et al., 2016; Jimura et al., 2013; Quiroz et al., 2016; Sesack and Grace, 2010; van den Bos et al., 2014). This suggests that compromised cortico-striatal regulation may drive heightened value-related striatal responses in psychopathy. If this is the case, weaker NAcc-vmPFC functional connectivity should be linked to stronger NAcc SV-related BOLD signal responses during intertemporal choice. To test this prediction, we examined correlations between NAcc SV-related BOLD signal and NAcc-vmPFC intrinsic connectivity strength across all subjects. Consistent with our supposition, we observed a negative relationship between NAcc-vmPFC functional connectivity and NAcc BOLD signal during intertemporal decision making (Figure 3; $r = -0.382$, $p = 0.011$). A significant relationship between NAcc-vmPFC rsFC and NAcc BOLD was also observed using robust regression ($t = -2.41$, $p = 0.021$), after excluding high-influence cases ($t = -2.25$, $p = 0.03$) and after controlling for age and substance abuse history ($t = -2.88$, $p = 0.006$; see Table S2). These results show that, across subjects, as NAcc-vmPFC connectivity strength decreases, the magnitude of NAcc value-related activity during choice behavior increases. This finding is consistent with a wealth of prior work indicating an important role for medial PFC in regulating ventral striatal function (Ferenczi et al., 2016; Haber et al., 1995; Quiroz et al., 2016; Sesack and Grace, 2010).

Cortical Regulation of Striatal Value Signaling Is Compromised in Psychopathy

The findings above show that psychopathy is associated with heightened striatal reactivity to the subjective value of choice options during intertemporal decision making; that ventromedial cortico-striatal functional connectivity is weaker in participants with high levels of psychopathy; and that participants with weaker medial cortico-striatal functional connectivity exhibit more robust striatal subjective value signals during choice. If the observed striatal hyper-reactivity in psychopathy is driven by compromised prefrontal regulation, then the negative relationship between cortico-striatal connectivity and SV-related striatal BOLD signal should be strongest in subjects with low PCL-R scores and weakest in participants with high PCL-R scores. In other words, cortico-striatal connectivity and striatal SV-related BOLD signal should progressively decouple with increasing psychopathy severity.

We tested this prediction using a conditional process (moderation) model constructed as follows: X = NAcc-vmPFC connectivity, Y = striatal SV BOLD, Moderator (M) = PCL-R score. The overall model was significant ($F = 3.316$, $p = 0.03$), as was the moderation term for PCL-R total scores ($r = 0.021$, 95% CI: 0.0005–0.0419; r^2 change = 0.088, $F = 4.30$, $p = 0.045$). To examine the conditional effect of X on Y at each level of M, we then decomposed this interaction using the Johnson-Neyman procedure. This analysis revealed that at low PCL-R scores (specifically, below 22), cortico-striatal connectivity was significantly negatively correlated with striatal SV BOLD (p value range: 0.007–0.05); however, as PCL-R scores increased above this threshold (i.e., >22) the relationship was no longer observed (Figure 4). To test the selectivity of this finding for vmPFC-striatal connectivity, we replaced these values with NAcc-precuneus connectivity estimates as the independent variable (X). Neither this model nor the moderation term was significant and no conditional effect of X on Y was observed (all $p > 0.05$). Factor-specific moderation analyses yielded similar results. Using Factor 1 (affective-interpersonal) PCL-R scores as the moderator, the overall model was significant ($F = 4.194$, $p = 0.011$), as was the moderation term ($\beta = 0.048$, 95% CI: 0.0046–0.0907; r^2 change = 0.097,

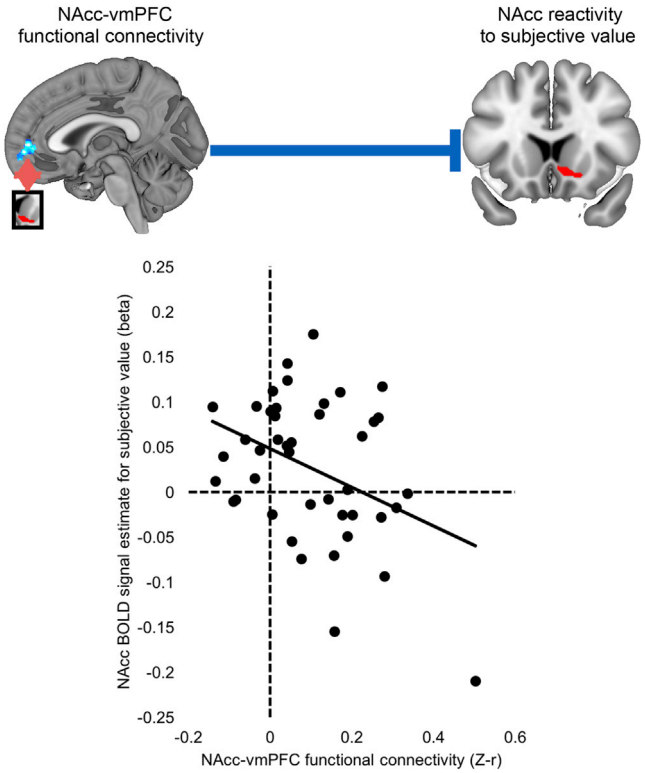

Figure 3. Cortico-striatal Connectivity as a Putative Regulator of Striatal Subjective Value-Related Activity

Scatterplot illustrates the significant negative correlation between NAcc-vmPFC functional connectivity and NAcc subjective value BOLD signal. Note: correlation remains significant after excluding high-influence data points.

F = 5.004, p = 0.031). Using Factor 2 (impulsive-antisocial) scores as the moderator, the overall model (F = 3.780, p = 0.018) and moderation term (β = 0.039, 95% CI: 0.0049–0.0739; r^2 change = 0.108, F = 5.336, p = 0.026) were likewise significant.

These analyses confirm that the relationship between cortico-striatal connectivity and value-related activity within NAcc varies as a function of psychopathy. Our data suggest that cortico-striatal connectivity negatively regulates striatal value signals in non-psychopathic individuals. However, this putative regulatory relationship is abolished in participants with high PCL-R scores—including those who meet consensus criteria for psychopathy (>30; see Hare and Neumann, 2008).

Cortico-striatal Circuit Dysfunction Tracks Variability in Criminal Behavior

The above findings suggest that striatal hyper-reactivity to the subjective value of choice options in psychopathy is driven by dysfunctional prefrontal regulation of striatal value signaling. Individuals who score high on the PCL-R show weakened functional connectivity between NAcc and ventromedial prefrontal cortex, and weaker connectivity, in turn, is linked to higher-magnitude striatal responses to the subjective value of reward options during decision making. To confirm that cortico-striatal circuit dysregulation translated into meaningful differences in real-world self-control, we examined whether individual differences in SV-related striatal activity and cortico-striatal connectivity were associated with variability in criminal behavior. Across all subjects, both stronger striatal value-related activation and weaker cortico-striatal connectivity were associated with a higher total number of convicted crimes (Figure 5; NAcc SV-related BOLD: z = 0.295, p = 0.049, NAcc-vmPFC connectivity: r = −0.395, p = 0.009). These relationships remained significant after controlling for age and substance abuse history (Table S2). Equivalent results were obtained using a robust regression model (t = 2.34, p = 0.024; t = 3.03, p = 0.004). In sum, heightened striatal BOLD signal amplitude and weaker NAcc-vmPFC rsFC—a pattern that is evident in individuals with high levels of psychopathy—predict higher levels of criminal behavior, a marker of maladaptive real-world decision making.

Main Effects of NAcc Resting-State Functional Connectivity

As a test of convergence, we examined estimates of cortico-striatal connectivity derived from "main effect" maps of striatal resting-state functional connectivity (rsFC) (i.e., the mean effect of connectivity across all participants). Main effect striatal rsFC networks were identified using the same anatomical NAcc ROI in which we found a significant association between PCL-R scores and striatal SV-related BOLD (Figure S3A). This analysis revealed significant rsFC between ventral striatum and ventromedial prefrontal cortex (Figure 3A; vmPFC; Brodmann Area [BA] 11/32). Additional suprathreshold foci encompassed aspects of perigenual cingulate (pgACC; BA 24/33), right dorsal ACC (dACC; BA 32), right dorsolateral PFC (dlPFC; BA 9), and left parahippocampal gyrus (PHG), as detailed in Table S1.

Correlations with Psychopathy, Striatal SV-Related BOLD Signal and Criminal Behavior

Standardized regression coefficients for each (main effect) suprathreshold cluster were estimated for each subject and correlated with their respective PCL-R scores. These values reflect the strength of intrinsic connectivity between striatum and the suprathreshold target region (e.g., vmPFC). NAcc-vmPFC rsFC was negatively correlated with total PCL-R scores (Figure S3B). In addition, we observed a nominally significant relationship between total PCL-R scores and striatal-pgACC connectivity (r = −0.357; p = 0.019) but this did not survive correction for the total number of suprathreshold target foci (0.05/5 = $p_{corrected}$ < 0.01; Figure S3B). PCL-R scores were not significantly correlated with rsFC between striatum and the other three suprathreshold target foci (i.e., dACC, dlPFC, and PHG; all p > 0.05). Significant negative correlations with NAcc-vmPFC connectivity parameters were observed for both Factor 1 and Factor 2 scores (affective-interpersonal: r = −0.352, p = 0.022; impulsive-antisocial: r = −0.392, p = 0.011). A significant relationship between NAcc-vmPFC rsFC connectivity values and PCLR Total score was also observed using robust regression (t = −3.11, p = 0.003). Pearson correlation analysis revealed a significant association between NAcc-vmPFC rsFC values derived from the analysis above and striatal SV-related BOLD signal (r = −0.31, p < 0.05), and between main effect-derived NAcc-vmPFC rsFC values and criminal incarceration (r = −0.39, p = 0.009). See Table S2 for additional details and controls.

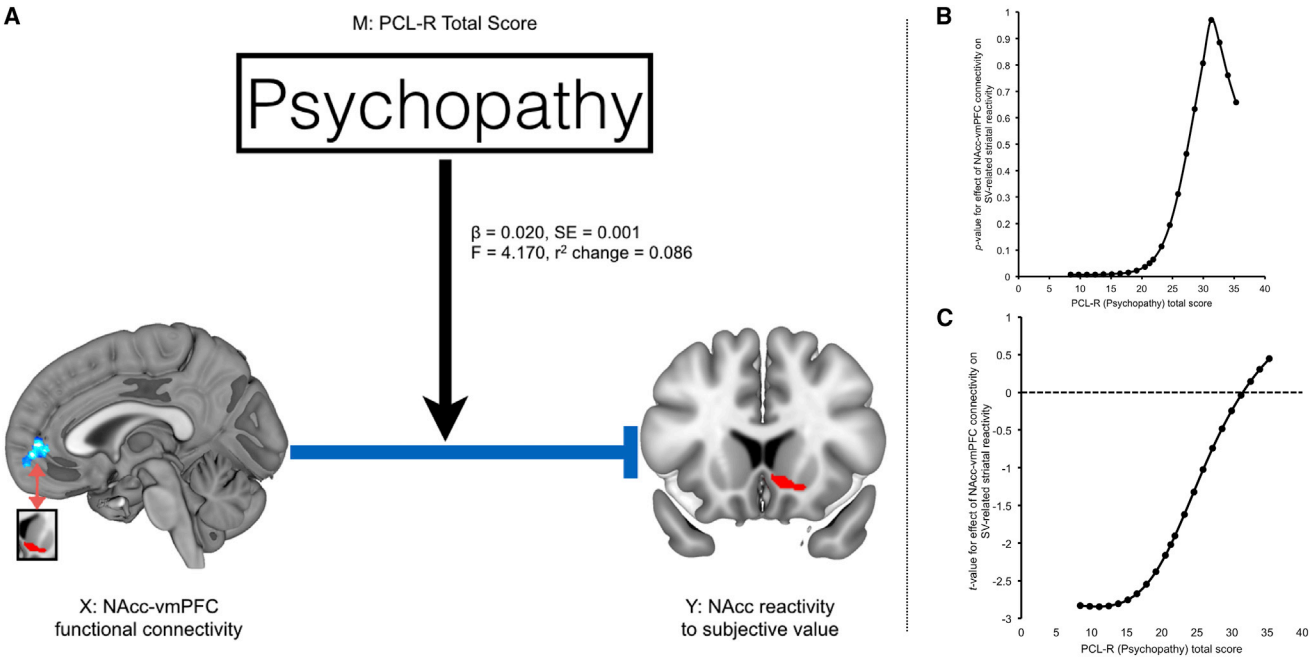

Figure 4. Psychopathy Moderates the Relationship between Cortico-striatal Connectivity and Value-Related BOLD Signal

(A) Schematic illustrates that PCL-R total scores significantly moderate the negative relationship between NAcc-vmPFC functional connectivity and SV-related NAcc BOLD signal.

(B and C) Johnson-Neyman p and t statistic values for the moderation regression analysis. At low psychopathy scores, NAcc-vmPFC connectivity strength was a negative predictor of NAcc BOLD responses to subjective value.

Moderation Analysis

A moderation model was constructed as follows: X = NAcc-vmPFC connectivity (derived from Main Effect rsFC map), Y = striatal SV BOLD, Moderator (M) = PCL-R score. The overall model was marginally significant ($F = 2.745$, $p = 0.056$). The moderation term for PCL-R Total score was significant ($\beta = 0.028$, 95% CI: 0.002–0.056; r^2 change = 0.088, $F = 4.154$, $p = 0.048$). In addition, separate moderation analyses were used to test for PCLR factor-selective effects. For Factor 1, the overall model was significant ($F = 3.94$, $p = 0.009$), as was the moderation term ($\beta = 0.064$, 95% CI: 0.008–0.120, r^2 change = 0.102, $F = 5.296$, $p = 0.027$). For Factor 2, the overall model was significant ($F = 2.995$, $p = 0.043$), as was the moderation term ($\beta = 0.05$, 95% CI: 0.002–0.098; r^2 change = 0.096, $F = 4.511$, $p = 0.04$). All moderation models controlled for the potentially confounding effects of age and substance abuse.

Associations with Log(k)

We ran a series of analyses that tested for associations between log(k) and PCLR score, striatal BOLD signal, NAcc-vmPFC rsFC, and criminal behavior. In each case, we estimated a linear regression model that considered log(k) as a predictor of PCLR, BOLD signal, rsFC, or criminal convictions. To account for heteroscedasticity, standard errors were calculated using the Huber-White sandwich estimator. Log(k) was not a significant predictor of PCLR total scores, striatal BOLD signal or criminal convictions (all p values > 0.2). Swapping the predictor with the DV (e.g., a model in which PCLR predicted log(k)) did not reveal any significant relationships (all p values > 0.2). We did however observe a trend-level relationship between log(k) and cortico-striatal rsFC, such that steeper discounting was associated with reduced NAcc-vmPFC coupling at rest ($p = 0.078$).

Control Analysis: Age and Substance Abuse History

To control for the potentially confounding effects of age and substance abuse, we ran a series of partial correlation analyses using age and cumulative years of substance abuse (derived from the Addiction Severity Index) as covariates of no interest. One participant, who had an ASI cumulative score of 76—corresponding to a Z score of 3.94—was excluded from covariate analyses due to concerns about reporting accuracy. After controlling for these potential confounds, the association between NAcc SV-related BOLD and PCL-R Factor 1 remained significant ($p = 0.026$); however, the relationship with PCL-R Total Scores and with PCL-R Factor 2 scores did not (PCL-R Total: $p = 0.105$; PCL-R Factor 2: $p = 0.344$). With respect to NAcc-vmPFC connectivity, controlling for age and substance abuse history had no effect on the strength of the observed correlations with PCL-R total scores ($p = 0.00009$), PCL-R Factor 1 scores ($p = 0.006$), or PCL-R Factor 2 scores ($p = 0.0004$). This was also the case when examining correlations with NAcc-vmPFC connectivity values derived from the main effect rsFC map (PCL-R total: $p = 0.002$; Factor 1: $p = 0.025$; Factor 2: $p = 0.005$). Likewise, controlling for age and substance abuse had no effect on the relationship between NAcc-vmPFC

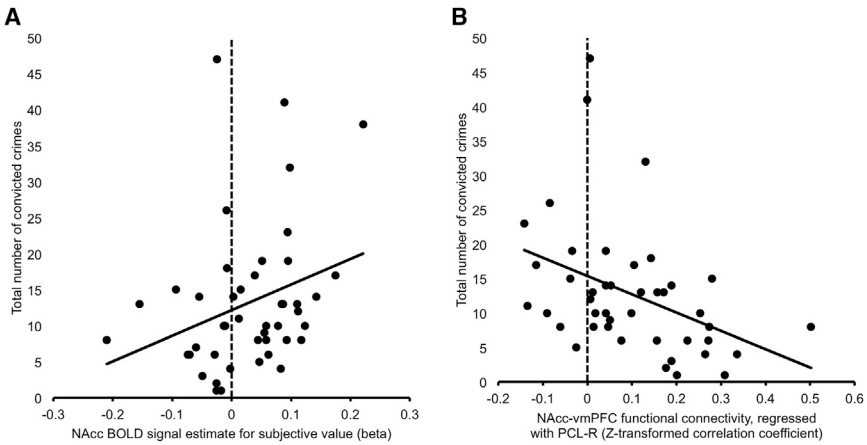

Figure 5. Stronger SV-Related BOLD Signal and Weaker NAcc-VMPFC rsFC Predict Higher levels of Criminal Behavior

(A) Scatterplot depicts the positive correlation between NAcc SV-related BOLD signal and total number of convicted crimes.

(B) Scatterplot depicts the negative correlation between NAcc-vmPFC functional connectivity and total number of convicted crimes.

connectivity and NAcc BOLD ($p = 0.009$ for psychopathy regression map estimate; $p = 0.002$ for main effect estimate), nor on the association between criminal convictions and NAcc BOLD ($p = 0.034$) or NAcc-vmPFC connectivity ($p = 0.012$ for psychopathy regression map; $p = 0.018$ for main effect rsFC map). The reported moderation analyses used age and substance-abuse adjusted data. See Table S2 for comprehensive output of all control analyses.

Selectivity Analysis: Striatal Subregions

We focused on ventral striatum due to prior reports implicating its role in reward-related decision making and potential dysfunction in psychopathy (Buckholtz et al., 2010; Glenn et al., 2010). This ventral striatal ROI was derived from a robust, large-scale ($n > 1,000$) study of striatal rsFC, wherein striatal subregions were differentiated based on their distinct patterns of intrinsic connectivity with cortical regions (Choi et al., 2012). The NAcc ROI used in the current study was one of seven ROIs identified in that work. To characterize the regional specificity of our observed correlations with psychopathy, we performed a series of correlation analyses using the remaining six striatal ROIs that encompassed medial caudate, lateral caudate and putamen (pre-commissural), and post-commissural putamen (Figure S4). Only SV-related BOLD signal within the right NAcc was significantly correlated with PCL-R scores, as discussed above; BOLD signal values within the other six striatal ROIs showed no association with total, Factor 1, or Factor 2 PCL-R scores, nor with total number of convicted crimes (all $p > 0.05$).

Selectivity Analysis: Decision Variables

The decision variable used to identify subjective value encoding regions in the striatum corresponds to the combined subjective value of the chosen and unchosen options (i.e., SV_{Sum}). This is but one of several potentially meaningful decision variables; others are sensitive to the difference in subjective value between the two choice options, and the subjective value chosen, unchosen, sooner-but-smaller, and larger-but-later choice options (respectively). To assess the selectivity of the observed associations with SV_{Sum}, we generated those alternative variables, input them as parametric modulators of BOLD signal at choice, and extracted the resulting parameter estimates from our NAcc ROI for each subject. We then tested for association with psychopathy and cortico-striatal rsFC in three ways. First, we looked at pairwise correlations. Of the decision variables tested (SV_{Sum}, $SV_{Difference}$ SV_{Chosen}, $SV_{Unchosen}$, SV_{SS}, SS_{LL}), only SV_{Sum} was found to be significantly correlated with PCLR scores (p value range for other decision variables: 0.194–0.778) or with cortico-striatal rsFC values (p value range for other decision variables: 0.139–0.830). Next, we used a multivariate analysis of variance (MANOVA) to account for the covariance in striatal signal between each decision variable. NAcc Striatal BOLD signal estimates associated with each decision variable were considered as dependent variables; PCLR scores and cortico-striatal rsFC values were considered as independent variables in two separate models. For the PCLR model, only SV_{Sum}-related BOLD signal was significantly predicted by PCLR scores (p value range for other decision variables: 0.194–0.554). Likewise, for the cortico-striatal rsFC model, only SV_{Sum}-related BOLD signal was significantly predicted by rsFC values (p value range for other decision variables: 0.139–0.820). Finally, we ran a series of partial correlations. Each model considered the relationship between SV_{Sum} and either PCLR score or cortico-striatal rsFC controlling for striatal BOLD signal estimates associated with $SV_{Difference}$ SV_{Chosen}, $SV_{Unchosen}$, SV_{SS}, or SS_{LL}. We found that the association between PCLR and striatal SV_{Sum}-BOLD remained significant even after controlling for striatal activity associated with each of these decision variables (range of p values for PCLR-BOLD relationship: 0.025–0.043; all r values were positively signed). Likewise, a significant negative relationship between cortico-striatal rsFC and SV_{Sum}-related striatal BOLD signal was observed even after adjusting for striatal activity linked to $SV_{Difference}$ SV_{Chosen}, $SV_{Unchosen}$, SV_{SS}, or SS_{LL} (range of p values: 0.013–0.040; all r values were negatively signed).

DISCUSSION

Psychopaths are aggressive and impulsive, exhibit poor behavioral controls, lack realistic long-term goals, and fail to accept responsibility for their severely antisocial behavior. These symptoms point to profound deficits in decision making, particularly when the future costs of an action must be reconciled with its immediate benefits. Here, we use a multi-modality imaging strategy in a sample of incarcerated offenders to detail a specific circuit-level mechanism that may account for such deficits in

decision making. Specifically, we show that psychopathy is associated with heightened ventral striatal subjective value signaling and compromised medial cortico-striatal functional connectivity. Across subjects, weaker connectivity was linked to stronger striatal value signaling, suggesting that cortico-striatal connectivity modulates the magnitude of such signals. Importantly, psychopathy significantly moderated the relationship between cortico-striatal connectivity and value-related activity within the striatum; at higher levels of psychopathy, the putative regulation of striatal value representations by NAcc-vmPFC connectivity was disrupted. Finally, the pattern of dysfunction evident in participants with high levels of psychopathy predicted the number of criminal convictions across subjects, providing a link to real-world maladaptive decision making.

These findings build on a growing body of prior work suggesting that psychopathy is associated with increased striatal gray matter volume and heightened reward-related NAcc activation (Bjork et al., 2010; Buckholtz et al., 2010; Glenn et al., 2010; Schiffer et al., 2011). The current findings converge to support the notion that striatal valuation signals are dysregulated in psychopathy and extend prior work in this area by demonstrating the relevance of these signals for decision making. Taken together, these data confirm the generalizability of prior associations in convenience samples to individuals with clinically relevant levels of psychopathy, reveal the circuit-level mechanisms driving striatal dysregulation, and link cortico-striatal dysregulation and striatal hyper-reactivity to maladaptive decision making in the real world.

Our finding of aberrant striatal connectivity with vmPFC is especially interesting considering prior reports of vmPFC dysfunction in psychopathy. Broadly, this literature provides evidence of reduced vmPFC activation during a range of tasks that tap aspects of moral decision making, empathic response, fear conditioning, affective processing, and norm-based cooperation (Birbaumer et al., 2005; Buckholtz, 2015; Decety et al., 2014, 2013b; Harenski et al., 2010). Studies of brain morphology suggest a structural origin for these findings: reduced cortical thickness, gyrification, and surface area within vmPFC have all been reported in adult psychopaths and in conduct-disordered youth with callous-unemotional traits (Ermer et al., 2012; Wallace et al., 2014). Several groups have also reported reduced white matter integrity within the uncinate fasciculus, a white matter tract that is principally responsible for information flow between vmPFC and striatum (as well as aspects of anterior and medial temporal lobe) (Motzkin et al., 2011; Sarkar et al., 2016; Wolf et al., 2015). Reduced vmPFC volume and uncinate fasciculus integrity could explain, in part, our finding of compromised cortico-striatal connectivity. Of note, prior observations of aberrant vmPFC structure and function in psychopathy have largely focused on the role of this region in social and affective processing. While a large body of work has shown that vmPFC is critical for representing value during decision making (Kable and Glimcher, 2009; O'Doherty, 2011), this is, to our knowledge, the first report linking vmPFC dysfunction in psychopathy to dysregulated value-based choice behavior and self-control.

The apparent disruption of vmPFC-NAcc connectivity in psychopathy is particularly intriguing given evidence that that vmPFC encodes value representations for delayed outcomes (Economides et al., 2015), possibly via model-based prospective simulations (Hampton et al., 2006; Peters and Büchel, 2010). We have suggested previously (Baskin-Sommers et al., 2016; Buckholtz, 2015) that the output of such model-based computations—which incorporate rule, context, and cost information—promotes adaptive behavior by modulating the ability of reward-associated cues to drive action selection via phasic dopamine (DA) signaling. The present finding that vmPFC-NAcc connectivity is inversely correlated with the magnitude of striatal value-related reactivity is consistent with this hypothesis and accords well with data showing that prefrontal afferents negatively regulate striatal DA transmission and population activity (Ferenczi et al., 2016; Quiroz et al., 2016). NAcc receives dense innervation from medial prefrontal cortex, and these cortico-striatal terminals are co-localized with midbrain DA projections (Haber and Knutson, 2010; Haber et al., 1995; Sesack and Grace, 2010). It has been proposed that prefrontal dysfunction leads to increased striatal DA transmission and reward-related striatal neuron firing by impairing the negative regulation of phasic DA release by PFC (Buckholtz, 2015; Casey et al., 2013). The current results provide convergent, translational support for the idea that higher-order value information maintained in prefrontal cortex impacts choice behavior by modulating striatal action value signals. In such a model, weaker model-based cortical modulation of model-free striatal value signals would impair adaptive behavior by limiting the ability of goal-based prospective representations to adaptively reweight action values.

The decision variable used to identify subjective value encoding regions in the striatum corresponds to the combined subjective value of the chosen and unchosen options (i.e., SV_{Sum}). It is important to note that this is but one of several potentially meaningful decision variables. Others are sensitive to the difference in subjective value between the two choice options, and the subjective value of chosen, unchosen, sooner-but-smaller, and larger-but-later choice options. We did not find any association between striatal BOLD signal linked to any of these decision variables and any of our clinical, connectivity, or behavioral measures. With that said, it was not our intention to make a strong claim about which specific decision variables were driving striatal value encoding in psychopaths. Rather, our goal was to precisely estimate preferences so that we could model exactly what the rewards on each trial were worth to each subject and derive estimates of brain signal corresponding to that valuation. The use of SV_{Sum} accomplishes this aim. Future work on delay discounting and other forms of value-based decision making in relevant populations might consider the use of task designs that better orthoganalize distinct components of valuation (Hare et al., 2008). Such designs would enable a more granular test of selectivity between facets of antisocial behavior and specific decision variables.

Contrary to our expectations, abnormal SV-related striatal activity and diminished striatal-prefrontal connectivity were not specific to the impulsive-antisocial component of psychopathy. Indeed, the association with NAcc BOLD signal was descriptively stronger for the interpersonal-affective dimension of psychopathy. This apparent lack of specificity may reflect the fact that deficits in impulse control are not easily attributable to a

single factor of psychopathy, but rather encompass both affective (lack of remorse, failure to accept responsibility for previous actions; Factor 1) and impulsive (failure to inhibit prepotent responses, need for stimulation; Factor 2) dimensions. Consistent with this, PCL-R total, PCL-R Factor 1, and PCL-R Factor 2 were each positively correlated with several trait measures of impulsivity (Table S3). In addition, though speculative, it is possible that the broad pattern of association we observe may reflect a shared role for vmPFC function and connectivity in aspects of cognition that jointly underlie socio-affective functioning and value-based decision making. vmPFC has been implicated in moral cognition (Koenigs et al., 2007), empathic responsiveness (Shamay-Tsoory et al., 2005), and theory of mind (Sebastian et al., 2012), as well as model-based prospective calculations of future outcome value (Hampton et al., 2006; Howard et al., 2015). It has been suggested (Buckner et al., 2008) that vmPFC—in concert with other nodes of the so-called default mode network—is critical for generating the dynamic mental simulations that are required for both perspective-taking (simulating another agent's mental state) and model-based prospective calculations (simulating future outcomes). It may be the case that by degrading the capacity for mental simulations, vmPFC dysfunction impairs both processes; in this way, aberrant vmPFC function and connectivity could constitute a common diathesis for the interpersonal-affective and impulsive-antisocial facets of psychopathy.

We note that our functional imaging studies are unable to resolve the specific neurochemical mechanisms underlying the apparent modulation of striatal activity by vmPFC. Further, our correlational findings cannot make claims about directionality and causal influence. Though unlikely given the known anatomy of the circuit (Haber and Knutson, 2010; Haber et al., 1995), it is possible that our observation of reduced cortico-striatal functional connectivity reflects impaired ascending information flow (i.e., modulation of vmPFC by NAcc through, for example, the ventral pallidum or thalamus). Alternatively, exaggerated midbrain dopamine neuron firing could lead to diminished vmPFC function (Arnsten, 2009) and/or potentiated NAcc DA efflux (Bello et al., 2011). However, we did not find any evidence for a relationship between psychopathy and midbrain function or connectivity in the current study. Future work employing neuroreceptor imaging, magnetic resonance spectroscopy, and causal manipulations such as non-invasive brain stimulation will be required to provide compelling empirical support for our circuit-level hypotheses. Nevertheless, taken together, the current data raise the intriguing possibility that vmPFC dysfunction—a robust finding in psychopathic populations—predisposes antisocial behavior by disrupting the cortical modulation of striatal value representations and highlight the importance of considering alterations in value-based decision-making as a proximal mechanism underlying self-control deficits in disinhibitory syndromes (Baskin-Sommers et al., 2016; Buckholtz et al., 2017).

STAR★METHODS

Detailed methods are provided in the online version of this paper and include the following:

- KEY RESOURCES TABLE
- CONTACT FOR REAGENT AND RESOURCE SHARING
- EXPERIMENTAL MODEL AND SUBJECT DETAILS
- METHOD DETAILS
  - Psychopathy Assessment
  - Inter-temporal Choice Task
  - MRI Acquisition
- QUANTIFICATION AND STATISTICAL ANALYSIS
  - fMRI Inter-Temporal Choice Task Analysis
  - rsFC MRI Analysis
  - Correlation, Moderation and Robust Regression Analyses

SUPPLEMENTAL INFORMATION

Supplemental Information includes four figures and three tables and can be found with this article online at http://dx.doi.org/10.1016/j.neuron.2017.06.030.

AUTHOR CONTRIBUTIONS

Conceptualization: J.W.B.; Methodology: E.K.K., G.R.S.-L., J.W.B.; Formal Analysis: J.G.H., E.K.K., J.W.B.; Investigation: E.K.K., H.M.D., J.W.B.; Resources: K.A.K., J.P.N.; Data Curation: E.K.K.; Writing – Original Draft: J.G.H., E.K.K., J.W.B.; Writing – Review and Editing: J.G.H., E.K.K., H.M.D., G.R.S.-L., A.B.-S., K.A.K., J.P.N., J.W.B.; Supervision: J.W.B.; Project Administration: A.B.-S., K.A.K., J.P.N., J.W.B.

ACKNOWLEDGMENTS

The authors are grateful to the Sloan Foundation (BR2013-018), the Brain and Behavior Research Foundation (21523), the Center for Law, Brain and Behavior at Massachusetts General Hospital, and the Canadian Institutes of Health Research for funding support.

Received: June 27, 2016
Revised: May 10, 2017
Accepted: June 16, 2017
Published: July 5, 2017

REFERENCES

Anderson, D.A. (1999). The Aggregate Burden of Crime. J. Law Econ. *42*, 611–642.

Arnsten, A.F. (2009). Stress signalling pathways that impair prefrontal cortex structure and function. Nat. Rev. Neurosci. *10*, 410–422.

Bartra, O., McGuire, J.T., and Kable, J.W. (2013). The valuation system: a coordinate-based meta-analysis of BOLD fMRI experiments examining neural correlates of subjective value. Neuroimage *76*, 412–427.

Baskin-Sommers, A., Stuppy-Sullivan, A.M., and Buckholtz, J.W. (2016). Psychopathic individuals exhibit but do not avoid regret during counterfactual decision making. Proc. Natl. Acad. Sci. USA *113*, 14438–14443.

Bello, E.P., Mateo, Y., Gelman, D.M., Noaín, D., Shin, J.H., Low, M.J., Alvarez, V.A., Lovinger, D.M., and Rubinstein, M. (2011). Cocaine supersensitivity and enhanced motivation for reward in mice lacking dopamine D2 autoreceptors. Nat. Neurosci. *14*, 1033–1038.

Birbaumer, N., Veit, R., Lotze, M., Erb, M., Hermann, C., Grodd, W., and Flor, H. (2005). Deficient fear conditioning in psychopathy: a functional magnetic resonance imaging study. Arch. Gen. Psychiatry *62*, 799–805.

Bjork, J.M., Chen, G., Smith, A.R., and Hommer, D.W. (2010). Incentive-elicited mesolimbic activation and externalizing symptomatology in adolescents. J. Child Psychol. Psychiatry *51*, 827–837.

Bjork, J.M., Chen, G., and Hommer, D.W. (2012). Psychopathic tendencies and mesolimbic recruitment by cues for instrumental and passively obtained rewards. Biol. Psychol. *89*, 408–415.

Blair, R.J. (2008). The amygdala and ventromedial prefrontal cortex: functional contributions and dysfunction in psychopathy. Philos. Trans. R. Soc. Lond. B Biol. Sci. *363*, 2557–2565.

Blair, R.J. (2013). The neurobiology of psychopathic traits in youths. Nat. Rev. Neurosci. *14*, 786–799.

Brazil, I.A., van Dongen, J.D., Maes, J.H., Mars, R.B., and Baskin-Sommers, A.R. (2016). Classification and treatment of antisocial individuals: From behavior to biocognition. Neurosci. Biobehav. Rev. Published online October 17, 2016. http://dx.doi.org/10.1016/j.neubiorev.2016.10.010.

Buckholtz, J.W. (2015). Social Norms, Self-Control, and the Value of Antisocial Behavior. Curr. Opin. Behav. Sci. *3*, 122–129.

Buckholtz, J.W., Treadway, M.T., Cowan, R.L., Woodward, N.D., Benning, S.D., Li, R., Ansari, M.S., Baldwin, R.M., Schwartzman, A.N., Shelby, E.S., et al. (2010). Mesolimbic dopamine reward system hypersensitivity in individuals with psychopathic traits. Nat. Neurosci. *13*, 419–421.

Buckholtz, J.W., Karmarkar, U., Ye, S., Brennan, G.M., and Baskin-Sommers, A. (2017). Blunted Ambiguity Aversion During Cost-Benefit Decisions in Antisocial Individuals. Sci. Rep. *7*, 2030.

Buckner, R.L., Andrews-Hanna, J.R., and Schacter, D.L. (2008). The brain's default network: anatomy, function, and relevance to disease. Ann. N Y Acad. Sci. *1124*, 1–38.

Cai, X., Kim, S., and Lee, D. (2011). Heterogeneous coding of temporally discounted values in the dorsal and ventral striatum during intertemporal choice. Neuron *69*, 170–182.

Carré, J.M., Hyde, L.W., Neumann, C.S., Viding, E., and Hariri, A.R. (2013). The neural signatures of distinct psychopathic traits. Soc. Neurosci. *8*, 122–135.

Casey, K.F., Cherkasova, M.V., Larcher, K., Evans, A.C., Baker, G.B., Dagher, A., Benkelfat, C., and Leyton, M. (2013). Individual differences in frontal cortical thickness correlate with the d-amphetamine-induced striatal dopamine response in humans. J. Neurosci. *33*, 15285–15294.

Choi, E.Y., Yeo, B.T., and Buckner, R.L. (2012). The organization of the human striatum estimated by intrinsic functional connectivity. J. Neurophysiol. *108*, 2242–2263.

Coid, J., Yang, M., Ullrich, S., Roberts, A., and Hare, R.D. (2009). Prevalence and correlates of psychopathic traits in the household population of Great Britain. Int. J. Law Psychiatry *32*, 65–73.

Decety, J., Chen, C., Harenski, C., and Kiehl, K.A. (2013a). An fMRI study of affective perspective taking in individuals with psychopathy: imagining another in pain does not evoke empathy. Front. Hum. Neurosci. *7*, 489.

Decety, J., Skelly, L.R., and Kiehl, K.A. (2013b). Brain response to empathy-eliciting scenarios involving pain in incarcerated individuals with psychopathy. JAMA Psychiatry *70*, 638–645.

Decety, J., Skelly, L., Yoder, K.J., and Kiehl, K.A. (2014). Neural processing of dynamic emotional facial expressions in psychopaths. Soc. Neurosci. *9*, 36–49.

Economides, M., Guitart-Masip, M., Kurth-Nelson, Z., and Dolan, R.J. (2015). Arbitration between controlled and impulsive choices. Neuroimage *109*, 206–216.

Ermer, E., Cope, L.M., Nyalakanti, P.K., Calhoun, V.D., and Kiehl, K.A. (2012). Aberrant paralimbic gray matter in criminal psychopathy. J. Abnorm. Psychol. *121*, 649–658.

Ferenczi, E.A., Zalocusky, K.A., Liston, C., Grosenick, L., Warden, M.R., Amatya, D., Katovich, K., Mehta, H., Patenaude, B., Ramakrishnan, C., et al. (2016). Prefrontal cortical regulation of brainwide circuit dynamics and reward-related behavior. Science *351*, aac9698.

Frick, P.J., and Viding, E. (2009). Antisocial behavior from a developmental psychopathology perspective. Dev. Psychopathol. *21*, 1111–1131.

Glenn, A.L., Raine, A., and Schug, R.A. (2009). The neural correlates of moral decision-making in psychopathy. Mol. Psychiatry *14*, 5–6.

Glenn, A.L., Raine, A., Yaralian, P.S., and Yang, Y. (2010). Increased volume of the striatum in psychopathic individuals. Biol. Psychiatry *67*, 52–58.

Goodall, C. (1983). M-estimators of Location: An Outline of the Theory, Vol. 5 (Wiley).

Gorgolewski, K., Burns, C.D., Madison, C., Clark, D., Halchenko, Y.O., Waskom, M.L., and Ghosh, S.S. (2011). Nipype: a flexible, lightweight and extensible neuroimaging data processing framework in python. Front. Neuroinform. *5*, 13.

Haber, S.N., and Knutson, B. (2010). The reward circuit: linking primate anatomy and human imaging. Neuropsychopharmacology *35*, 4–26.

Haber, S.N., Kunishio, K., Mizobuchi, M., and Lynd-Balta, E. (1995). The orbital and medial prefrontal circuit through the primate basal ganglia. J. Neurosci. *15*, 4851–4867.

Hampton, A.N., Bossaerts, P., and O'Doherty, J.P. (2006). The role of the ventromedial prefrontal cortex in abstract state-based inference during decision making in humans. J. Neurosci. *26*, 8360–8367.

Hare, R.D., and Neumann, C.S. (2008). Psychopathy as a clinical and empirical construct. Annu. Rev. Clin. Psychol. *4*, 217–246.

Hare, T.A., O'Doherty, J., Camerer, C.F., Schultz, W., and Rangel, A. (2008). Dissociating the role of the orbitofrontal cortex and the striatum in the computation of goal values and prediction errors. J. Neurosci. *28*, 5623–5630.

Harenski, C.L., Harenski, K.A., Shane, M.S., and Kiehl, K.A. (2010). Aberrant neural processing of moral violations in criminal psychopaths. J. Abnorm. Psychol. *119*, 863–874.

Howard, J.D., Gottfried, J.A., Tobler, P.N., and Kahnt, T. (2015). Identity-specific coding of future rewards in the human orbitofrontal cortex. Proc. Natl. Acad. Sci. USA *112*, 5195–5200.

Hyde, L.W., Byrd, A.L., Votruba-Drzal, E., Hariri, A.R., and Manuck, S.B. (2014). Amygdala reactivity and negative emotionality: divergent correlates of antisocial personality and psychopathy traits in a community sample. J. Abnorm. Psychol. *123*, 214–224.

Jimura, K., Chushak, M.S., and Braver, T.S. (2013). Impulsivity and self-control during intertemporal decision making linked to the neural dynamics of reward value representation. J. Neurosci. *33*, 344–357.

Kable, J.W., and Glimcher, P.W. (2009). The neurobiology of decision: consensus and controversy. Neuron *63*, 733–745.

Koenigs, M., Young, L., Adolphs, R., Tranel, D., Cushman, F., Hauser, M., and Damasio, A. (2007). Damage to the prefrontal cortex increases utilitarian moral judgements. Nature *446*, 908–911.

Koenigs, M., Baskin-Sommers, A., Zeier, J., and Newman, J.P. (2011). Investigating the neural correlates of psychopathy: a critical review. Mol. Psychiatry *16*, 792–799.

Motzkin, J.C., Newman, J.P., Kiehl, K.A., and Koenigs, M. (2011). Reduced prefrontal connectivity in psychopathy. J. Neurosci. *31*, 17348–17357.

O'Doherty, J.P. (2011). Contributions of the ventromedial prefrontal cortex to goal-directed action selection. Ann. N Y Acad. Sci. *1239*, 118–129.

Peters, J., and Büchel, C. (2010). Episodic future thinking reduces reward delay discounting through an enhancement of prefrontal-mediotemporal interactions. Neuron *66*, 138–148.

Peters, J., and Büchel, C. (2011). The neural mechanisms of inter-temporal decision-making: understanding variability. Trends Cogn. Sci. *15*, 227–239.

Quiroz, C., Orrú, M., Rea, W., Ciudad-Roberts, A., Yepes, G., Britt, J.P., and Ferré, S. (2016). Local Control of Extracellular Dopamine Levels in the Medial Nucleus Accumbens by a Glutamatergic Projection from the Infralimbic Cortex. J. Neurosci. *36*, 851–859.

Sarkar, S., Dell'Acqua, F., Froudist Walsh, S., Blackwood, N., Scott, S., Craig, M.C., Deeley, Q., and Murphy, D.G. (2016). A Whole-Brain Investigation of White Matter Microstructure in Adolescents with Conduct Disorder. PLoS ONE *11*, e0155475.

Schiffer, B., Müller, B.W., Scherbaum, N., Hodgins, S., Forsting, M., Wiltfang, J., Gizewski, E.R., and Leygraf, N. (2011). Disentangling structural brain

alterations associated with violent behavior from those associated with substance use disorders. Arch. Gen. Psychiatry *68*, 1039–1049.

Sebastian, C.L., Fontaine, N.M., Bird, G., Blakemore, S.J., Brito, S.A., McCrory, E.J., and Viding, E. (2012). Neural processing associated with cognitive and affective Theory of Mind in adolescents and adults. Soc. Cogn. Affect. Neurosci. *7*, 53–63.

Sesack, S.R., and Grace, A.A. (2010). Cortico-Basal Ganglia reward network: microcircuitry. Neuropsychopharmacology *35*, 27–47.

Shamay-Tsoory, S.G., Tomer, R., Berger, B.D., Goldsher, D., and Aharon-Peretz, J. (2005). Impaired "affective theory of mind" is associated with right ventromedial prefrontal damage. Cogn. Behav. Neurol. *18*, 55–67.

Skeem, J.L., and Mulvey, E.P. (2001). Psychopathy and community violence among civil psychiatric patients: results from the MacArthur Violence Risk Assessment Study. J. Consult. Clin. Psychol. *69*, 358–374.

van den Bos, W., Rodriguez, C.A., Schweitzer, J.B., and McClure, S.M. (2014). Connectivity strength of dissociable striatal tracts predict individual differences in temporal discounting. J. Neurosci. *34*, 10298–10310.

Viding, E., McCrory, E., and Seara-Cardoso, A. (2014). Psychopathy. Curr. Biol. *24*, R871–R874.

Wallace, G.L., White, S.F., Robustelli, B., Sinclair, S., Hwang, S., Martin, A., and Blair, R.J. (2014). Cortical and subcortical abnormalities in youths with conduct disorder and elevated callous-unemotional traits. J. Am. Acad. Child Adolesc. Psychiatry *53*, 456–65.e1.

Walters, G.D. (2003). Predicting institutional adjustment and recidivism with the psychopathy checklist factor scores: a meta-analysis. Law Hum. Behav. *27*, 541–558.

Wolf, R.C., Pujara, M.S., Motzkin, J.C., Newman, J.P., Kiehl, K.A., Decety, J., Kosson, D.S., and Koenigs, M. (2015). Interpersonal traits of psychopathy linked to reduced integrity of the uncinate fasciculus. Hum. Brain Mapp. *36*, 4202–4209.

Yang, Y., and Raine, A. (2009). Prefrontal structural and functional brain imaging findings in antisocial, violent, and psychopathic individuals: a meta-analysis. Psychiatry Res. *174*, 81–88.

STAR★METHODS

KEY RESOURCES TABLE

REAGENT or RESOURCE	SOURCE	IDENTIFIER
Software and Algorithms		
Nipype	Niypype Development Group	http://nipype.readthedocs.io/en/latest/
Statistical Parametric Mapping	Wellcome Trust, London	http://www.fil.ion.ucl.ac.uk/spm/software/spm8/
MATLAB	MathWorks	MATLAB R2015a
STATA	StataCorp	StataMP 14.2
SPSS Statistics	IBM	SPSS Statistics v24

CONTACT FOR REAGENT AND RESOURCE SHARING

Further information and requests for resources should be directed to the Lead Contact, Joshua W. Buckholtz (joshuabuckholtz@fas.harvard.edu).

EXPERIMENTAL MODEL AND SUBJECT DETAILS

Participants were 49 male incarcerated offenders recruited from two medium-security correctional institutions (Fox Lake Correctional Institute and Oshkosh Correctional Institution, Wisconsin). Criteria for eligibility were defined as follows: age 45 years old or younger (range = 20-45, mean = 31), IQ > 70, no history of psychosis or bipolar disorder, no history of concussion or post-concussive syndrome, and not concurrently taking psychotropic medications. 3 participants were excluded for exhibiting no behavioral variability, and 1 participant was excluded for excessive head motion during scanning (see below). Thus, 45 participants were included in the imaging analyses. We were not able to obtain rsFC data for two of these 45 subjects.

Following initial screening, participants were given a life-history interview (for use with the PCL-R assessment; see below), as well as a semi-structured interview for the Addiction Severity Index (ASI) and a structured psychiatric interview (SCID-NP). During the ASI, subjects were asked to indicate their years of substance use for every illicit drug they had used. The duration value for each substance (in years) was summed; this cumulative drug abuse score (range = 0-76, mean = 15) was used as a covariate in subsequent analyses.

Written informed consent was obtained for all participants, and all methods and procedures were approved by the University of New Mexico, University of Wisconsin-Madison, and Harvard University Institutional Review Boards.

METHOD DETAILS

Psychopathy Assessment

The Psychopathy Checklist-Revised (PCL-R), a ‘‘gold standard’’ clinical and forensic tool for assessing psychopathy, was administered to all participants. PCL-R ratings were performed by a trained rater and consisted of both a 60-90 min semi-structured interview and a review of collateral file material (e.g., charging documents, sentencing reports). Each participant was rated between 0-2 on 20 items, for a maximum possible score of 40. PCL-R scores fell within a range of 8 and 35, with a mean of 23.5. Inter-rater reliability was very high, at 0.96 for the 30% of the sample. The PCL-R subdivides into two correlated ‘‘factors,’’ with Factor 1 comprising Interpersonal and Affective deficits, and Factor 2 comprising Impulsive and Antisocial symptoms (Hare and Neumann, 2008). Total, Factor 1 and Factor 2 scores were calculated for each subject.

Inter-temporal Choice Task

During scanning (see below), participants performed a delay-discounting procedure that involved choosing between smaller-but-sooner (SS) and larger-but-later (LL) monetary rewards (Figure S1). SS options were immediate or delayed by 2 or 4 weeks, and LL options were either 2 or 4 weeks after the delay of the SS option; for all trials, LL delay was 2-8 weeks from scan day. SS reward magnitude on each trial was determined by sampling from a distribution bounded at $5 and $40 ($20 mean). LL rewards were 1%, 3%, 5%, 10%, 15%, 25%, 35%, or 50% greater than SS. To reduce interindividual variability in trial history and composition, we created a fixed trial order that was used for all participants (i.e., all subjects saw the same trials in the same order). Participants completed three ~8 min runs, each comprising 48 trials; total task time was thus approximately 24 min. Individuals were instructed that one of their choices would be randomly selected and paid into their prison commissary account at the end of the experiment, following its associated delay. Three participants who chose exclusively SS or LL options were excluded from subsequent analyses.

For each individual, choice data were used to estimate their delay discount rate (k) from a hyperbolic value function and the decision slope from a softmax decision function in MATLAB. Specifically, we applied the softmax choice rule to estimate the probability of choosing the sooner/smaller reward (P_{SS}) on each trial, given the subjective values of the sooner/smaller and larger/later rewards $(1/1+e^{-\beta(V_{SS}-V_{LL})})$. The free parameter β models the stochasticity of a given participants' choice behavior. Best-fitting parameter estimates for each subject were obtained via maximum-likelihood estimation with Nelder-Mead simplex optimization (implemented through the fminsearch function). To obtain the best-fitting model parameters for each model and subject, we maximized the log-likelihood (L-L) of the choice given a set of model parameters, summing across all trials for each subject. To avoid local minima, the estimation procedure was repeated with 100 random combinations of starting values for each model for each subject, keeping track of the overall maximum L-L. For the value function, we used the formula VS = VO / (1 + kD), where VS is the subjective value of a given option, VO is the reward magnitude of that option, D is the option's associated delay, and k is a free parameter that represents how steeply they discount the subjective value of a given option at increasing delays. Individuals with larger k values exhibit steeper discounting and are thus more intolerant to delay (i.e., more impulsive). Prior work has shown that the distribution of k values is skewed; to conform to the assumptions of the general linear model, k values were natural log-transformed for subsequent analysis of the behavioral data. The k values (not log transformed) were also used to estimate subjective value on each trial for neuroimaging analyses (see below).

MRI Acquisition

MR images were acquired on correctional facility grounds, using a Siemens 1.5 T Avanto Mobile MRI System with advanced SQ gradients (max slew rate 200 T/m/s, 346 T/m/s vector summation, rise time 200 μs) and equipped with a 12-channel head coil. Head motion was limited via padding and restraint.

Prior to all functional scans, a T1-weighted structural image was captured for each participant using a four-echo MPRAGE sequence (TR = 2530ms, TE = 1.64, 3.5, 5.36, and 7.22 ms; flip angle = 7°, FOV = 256 × 256 mm, matrix = 128x 128, slice thickness = 1.33 mm, no gap, voxel size = 1.0 × 1.0 × 1.33 mm, 128 interleaved sagittal slices per echo), with the four echoes averaged into a single high-resolution image.

Task-related fMRI data collection

The delay-discounting task was back-projected onto a screen at the front of the magnet bore, which participants viewed through a mirror positioned above them. Individuals indicated their choice by pressing the corresponding button on a MRI-compatible button box. While performing the task, functional (T2*-weighted) images were acquired via a gradient-echo echoplanar imaging (EPI) pulse sequence with the following parameters: TR = 2500 ms, TE = 39 ms, flip angle = 90°, FOV = 220 × 220 mm, matrix = 64 × 64, slice thickness = 3.4 mm, gap = 0.34 mm, voxel size = 3.4 × 3.4 × 3.4 mm, 33 interleaved axial oblique slices per volume.

Resting-state functional connectivity (rsFC) MRI data collection

Subjects lay still and awake, and were instructed to passively view a fixation cross while resting-state functional images were collected. Parameters for T2*-weighted gradient-echo EPIs were as follows: TR = 2500 ms, TE = 39 ms, flip angle = 90°, FOV = 220 × 220 mm, matrix = 64 × 64, slice thickness = 3.4 mm, gap = 1 mm, voxel size = 3.4 × 3.4 × 3.4 mm, 33 sequential axial oblique slices. Resting-state scans comprised 141 volumes, lasting 5.5 min. Resting-state was not able to be acquired for two subjects.

QUANTIFICATION AND STATISTICAL ANALYSIS

fMRI Inter-Temporal Choice Task Analysis

All imaging data were analyzed using SPM8 (SPM, FIL Methods Group, Wellcome Trust Centre for Neuroimaging, London, UK), implemented in MATLAB (MathWorks, Sherborn, MA) and Nipype (Gorgolewski et al., 2011), using Harvard University's Neuroimaging Compute Facility cluster and Apple personal computers.

Preprocessing

Prior to analysis, task-related functional images were slice-time corrected using the first slice as a reference, and motion corrected via spatial realignment (2nd-degree B-spline) of all images to a mean image after alignment to the first image of each run. Images were then spatially normalized using unified segmentation and normalization, via the NewSegment routine in SPM, into a standard stereotactic space (Montreal Neurological Institute, MNI template), resampled into 2mm isotropic voxels, and smoothed with a 6mm full-width-half-maximum Gaussian kernel. A high-pass filter (128 s cutoff) was applied to remove low-frequency signal drift. Runs were removed if they had a total rotational plus translational displacement of 1 mm or a mean-signal score > 3 standard deviations from the norm, using Artifact Detect in Nipype. Participants with fewer than two usable runs were removed completely. Using these criteria resulted in the exclusion of one participant due to excessive head motion during scanning.

First-level (single-subject) models

All trial types were pooled. Trials were modeled using a canonical hemodynamic response function (HRF) with a time derivative, onset at choice and duration of 0. Using participants' *k* values derived from the delay-discounting task, we estimated the subjective value of each of the two options presented on every trial. These values were summed to create a single "SV-Sum" variable for each trial, for

each participant. We modeled SV-Sum as a parametric modulator (pmod) of BOLD signal at the time of choice. A contrast of this pmod revealed regions whose activity tracked trial-wise variation in subjective value.

Second-level (group) analyses

The effect of subjective value on NAcc activity was estimated by entering each participant's first-level SV-Sum contrast into a random-effects general linear model (one-sample t test). The resulting SPM was corrected for multiple comparisons within an anatomical NAcc ROI (see below), with a peak-level false-discovery rate (FDR) set to $p < 0.05$.

Region-of-interest (ROI) extraction

The software ROI Extraction (REX), as implemented in MATLAB, was used to extract mean NAcc BOLD signal estimates from each participant's SV-Sum GLM. We chose an anatomical ROI derived from a 1000-subject resting-state functional connectivity-based parcellation of the striatum (Choi et al., 2012). One of the seven subregions delineated in that study (corresponding to "network 5" in Choi et al., 2012) corresponded with the anterior ventral striatum, i.e., nucleus accumbens; this ROI was chosen for our primary analyses. Other striatal ROIs in that parcellation encompassed aspects of the caudate and putamen, and were used for post hoc tests of regional selectivity.

rsFC MRI Analysis

Preprocessing

The resting-state functional connectivity preprocessing pipeline has been described in detail elsewhere (Choi et al., 2012). Briefly, a Gaussian filter was used to remove noise, a temporal bandpass filter was applied to select for the blood oxygen level-dependent (BOLD) frequency signal, and nuisance regressors were applied for (in order) head motion, whole-brain signal, white matter signal, and ventricular signal. Runs were removed if they had a total rotational plus translational displacement of 1mm or a mean-signal score > 3 standard deviations, using Artifact Detect in Nipype. Using these criteria, one participant was removed from the study due to excessive head motion during scanning. With signals of non-neuronal origin thus removed, including fluctuation due to respiration, seed-based connectivity maps could then be estimated.

Seed-based rsFC Analyses: Intrasubject Correlation Maps

Functional connectivity maps were created using a custom-built analysis pipeline, which incorporates both custom C programming and the neuroimaging package FSL, and has been described in detail elsewhere (Choi et al., 2012). Briefly, mean time course data were extracted from the NAcc ROI described above. Regressor data were modeled from these time course data and fit to the BOLD signal time course in each voxel across the brain using linear regression. These were converted to correlation coefficient images, and then transformed to z-maps to increase distribution normality for the images.

rsFC Main Effect Maps

Group-averaged whole-brain connectivity maps were generated via random-effects GLM analysis in SPM8, and corrected for multiple comparisons using a cluster-level FDR threshold of $p < 0.05$, in combination with a cluster-forming height threshold of $t > 3$. We extracted connectivity estimates for each suprathreshold cluster using spheres with a diameter of 15mm and centered on the cluster's peak voxel.

rsFC PCL-R Correlation Maps

As a complementary approach, we identified regions where rsFC with the striatal ROI varied as a function of PCL-R score. PCL-R scores were regressed against each individual's striatal rsFC contrast via random-effects GLM analysis in SPM8, and corrected for multiple comparisons using an FDR_{Peak} threshold of $p < 0.05$ (cluster-forming height threshold of $t > 3$).

Correlation, Moderation and Robust Regression Analyses

Trait correlation and moderation analyses were performed in SPSS (version 22; SPSS/IBM, Chicago, IL). These included bivariate, two-tailed, Pearson correlations for all clinical and behavioral measures, SV-related BOLD signal, and intrinsic functional connectivity estimates. Partial correlation analyses were used to control for the potentially confounding effects of age and drug use on striatal function and connectivity. Pearson r values with corresponding p values are provided in the Results Section.

Moderation analyses were performed with the SPSS macro PROCESS (Andrew F. Hayes, Ohio State University, Columbus, OH). We tested a model wherein X = NAcc-vmPFC connectivity, Y = NAcc SV-related BOLD, and M = PCL-R total score. A non-parametric resampling procedure (bootstrapping) with 5000 samples was used to estimate the significance of the moderation effect. Through bootstrapping, we calculated point estimates of the moderation effect over all samples, and constructed a 95% confidence interval around each point estimate. Statistical significance is inferred if the upper and lower bounds of the confidence interval do not contain zero. Bootstrapping is generally considered preferable to parametric tests, because it avoids the assumption of normality for the sampling distributions of the moderation effect, which is typically violated in practice. Statistical parameters reported in the Results section include the F values for the overall model, r2 change values, beta weight values for point estimates with corresponding confidence intervals, and p values.

Robust regression analyses were performed in Stata (version 14) using the *rreg* function. *rreg* first fits the OLS regression and calculates Cook's D for each case. Cases with $D > 1$ are excluded from subsequent analyses. Thereafter, rreg uses an iterative

re-weighting approach: case weights are calculated from the absolute residuals on each iteration, with each subsequent iteration employing those weights. Iterations stop when the maximum change in weights drops below tolerance (0.01). Both Huber and biweight weight functions are used in sequence: Huber until convergence, and then, from that result, biweights are used until convergence. In rreg, the Huber tuning constant is hard-coded to be 1.345, meaning that downweighting begins with cases where the absolute residual is greater than (1.345/0.6745)$M \approx 2M$, where M = median absolute deviation from the median residual. With biweighting, all cases with nonzero residuals receive some downweighting. In rreg, the 'aggressiveness' of this downweighting can be specified by the user. Goodall (1983) recommends a biweight tuning constant that drops (i.e., assigns a weight of 0 to) cases with absolute residuals exceeding $6M$-$9M$, inclusive. To achieve this, we set the tuning constant to 5.396, corresponding to a threshold of $\approx 8M$. t value and p values are reported for robust regression analyses in the Results section.